SCI. MAR., 65 (Suppl. 1): 269-276 SCIENTIA MARINA 2001

AN INTERDISCIPLINARY VIEW OF THE OCEAN. *J.L. PELEGRÍ, I. ALONSO and J. ARÍSTEGUI (eds.)*

Wind and tide current prediction using a 3D finite difference model in the Ría de Vigo (NW Spain)*

C. SOUTO[1], L. FARIÑA-BUSTO[1], E. ALVAREZ[2] and I. RODRÍGUEZ[2]

[1]Física de la Tierra, Facultad de Ciencias, Universidad de Vigo, Campus de Lagoas-Marcosende, 36200 Vigo. Spain.
[2]Área de Conocimiento y Análisis del Medio Físico, Ente Público Puertos del Estado, Avda. del Partenón 10, 28042 Madrid, Spain.

SUMMARY: A 3D barotropic finite difference model was adapted to reproduce the dynamics of the Ría de Vigo estuary, in the north-west corner of Spain. The model has been applied with astronomical tide and observed wind forcing data. The results are compared to data obtained by an AANDERAA DCM 12 acoustic Doppler current meter at one point of the Ría.

Key words: currents, finite difference model, estuaries, Ría de Vigo (NW Spain).

INTRODUCTION

The Ría de Vigo is an estuary located on the Atlantic coast of the north-west corner of Spain, and is the southernmost of the four which are often collectively referred to as the Galician Rías Baixas. It extends along 32 km in a NE-SW direction, opening steadily from 1 km width at the 20 m deep Rande Strait to about 10 km at the 40 m deep outer part. Beyond the Rande Strait the Ría closes in San Simón Bay, a very shallow area which collects most of the river runoff to the estuary. The Ría has an area of about 156 km^2 and a volume of approximately 3x10^9 m^3. It opens to the shelf through two mouths: the northern one is 2.5 km wide and has a maximum depth of 25 m and the southern one is 5 km wide and has a maximum depth of 50 m depth. In between both mouths are the two Cíes Islands (Fig. 1).

*Received October 4, 1999. Accepted July 14, 2000.

This work presents some results of a 3D finite difference circulation model applied to the Ría de Vigo which is capable of reproducing wind- and tide-generated currents. At intermediate frequencies, i.e. time scales of less than a day and more than two hours, the tidal dynamics is generally expected to be dominant. At lower frequencies wind forcing is likely to be the most important factor in determining currents. How good this statement is can be tested if the observed currents are well reproduced with only barotropic forcing, and no stratification is included in the simulation. The results presented here support this choice.

The model used is a C++ version of the HAMSOM model, originally developed by the Institut für Meereskunde Hamburg and the Programa de Clima Marítimo (PCM) (Backhaus, 1983, 1985; Backhaus and Hainbucher, 1987; Rodríguez and Alvarez, 1991; Rodríguez *et al.*, 1991; Stronach *et al.*, 1993). The C++ code is more compact (the number of code lines is about half that of its FORTRAN counter-

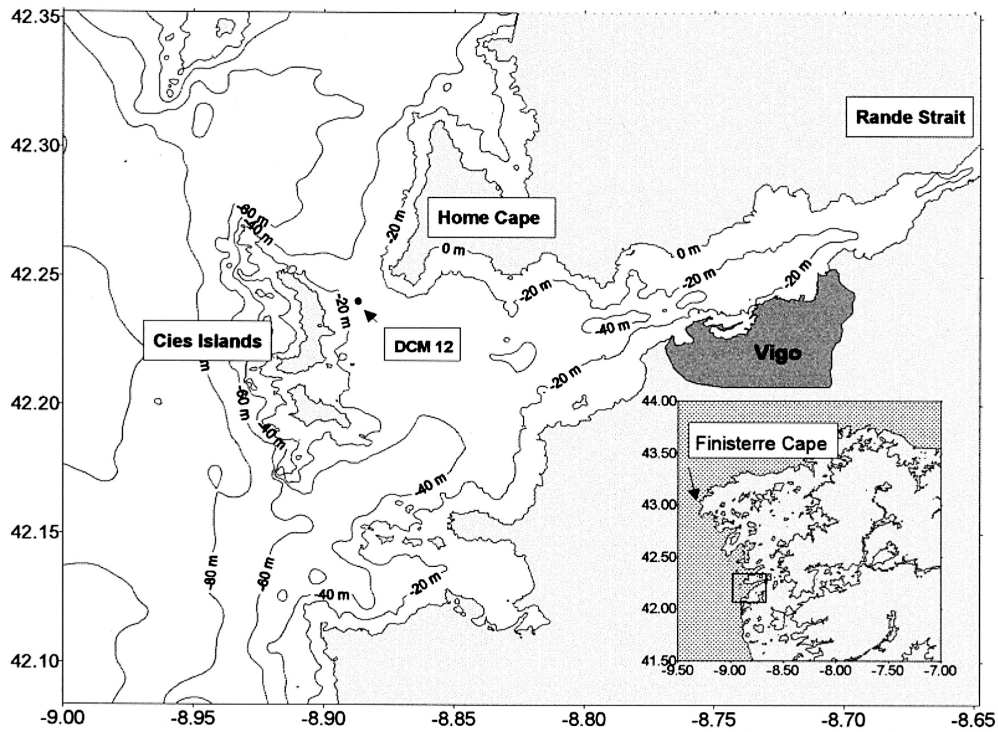

FIG. 1. – The bathymetry of the Ría de Vigo used in the simulation. The dot at the northern mouth indicates the point of deployment of the DCM 12.

part), more efficient and allows new code to be introduced more easily. A typical run with 44000 calculation points which allows cells of 300×300 m and 13 levels takes a quarter of an hour per day of simulation on a Pentium II-400 personal computer. To the authors' knowledge this is the first time that 3D numerical prediction model results have been directly compared to real current data in any of the Galician Rías.

The article is organised as follows. First the deployments of Doppler current meters are briefly described. A brief review of the finite difference HAMSOM model is given, and the grid, parameters and closure scheme used in the simulation as well as the characteristics of the forcing applied are explained. Then the results of the model are shown and compared to the real data. Finally, some conclusions are drawn in the discussion.

MATERIAL AND METHODS

The moorings

An AANDERAA Doppler Current Meter (DCM12) was deployed in exactly the same position in the sill of the northern mouth of the Ría, at 25 m depth (for the deployment an iron and cement structure was used to protect the DCM, which also ensured the exact location of the point) during two different periods, one in spring from 10/4/97 to 16/5/97 and one in autumn from 9/9/97 to 24/10/97. The AANDERAA DCM 12 is an acoustic current meter by Doppler effect. It divides the water column into five layers (which partially overlap) with centres uniformly distributed in the water column (in this case at approximately 3.5, 7, 11, 14 and 18 m). An averaged velocity for each layer, roughly 6 m thick, is then registered. A pressure sensor allows the tidal height to be measured. The time interval at which each sample was taken was set to ten minutes for the first deployment and thirty minutes for the second one, thus allowing a high time resolution.

The model

The HAMSOM model is a three-dimensional multi-level (z co-ordinate) finite difference baroclinic model (Arakawa C grid) based on Navier-Stokes equations with the hydrostatic approximation, mass continuity and equations for salt and temperature (which in this paper are not used since the study is restricted to constant density forcing). The basic equations here are:

$$\frac{\partial u}{\partial t} + u\frac{\partial u}{\partial x} + v\frac{\partial u}{\partial t} + w\frac{\partial u}{\partial z} + \frac{1}{\rho}\frac{\partial P}{\partial x} =$$

$$= fv + A_h\left[\frac{\partial^2 u}{\partial x^2} + \frac{\partial^2 u}{\partial y^2}\right] + \frac{\partial \tau_{xz}}{\partial z}$$

$$\frac{\partial u}{\partial t} + u\frac{\partial u}{\partial x} + v\frac{\partial u}{\partial t} + w\frac{\partial u}{\partial z} + \frac{1}{\rho}\frac{\partial P}{\partial y} =$$

$$= -fu + A_h\left[\frac{\partial^2 v}{\partial x^2} + \frac{\partial^2 v}{\partial y^2}\right] + \frac{\partial \tau_{yz}}{\partial z}$$

$$\frac{\partial P}{\partial z} = -pg$$

$$\frac{\partial u}{\partial x} + \frac{\partial v}{\partial y} + \frac{\partial w}{\partial z} = 0$$

where u, v and w are the Cartesian vector velocity components; t the time; P the pressure; g the Earth's acceleration; ρ the water density; f the Coriolis parameter; τ_{xz} and τ_{yz} components of the stress tensor and A_h the horizontal eddy viscosity (kept constant at 30 m^2/s). The vertical diffusion of velocity was calculated using a first order scheme based on the mixed layer length (Rodi, 1980), which is useful to reproduce the thermohaline fields.

The equations are discretised using a two-time level numerical scheme (Alvarez *et al.*, 1997), in which some terms (like pressure gradient or vertical diffusive stress) are dealt with semi-implicitly and others (momentum advection and horizontal diffusion) explicitly. The Coriolis term is calculated following the approach developed by Wais (1985).

The bathymetry used was obtained from charts of the Instituto Hidrográfico de la Marina, and discretised to a grid of square cells of 300×300 m. The oceanic western side of the model is located at a longitude of -9º. This border was selected so that a major part of the total volume of the grid was placed over the shelf, thus allowing upwelling and downwelling to occur within the Ría without much influence of the finiteness of the volume of integration. A zero-gradient condition was also imposed in order to further weaken the influence of the border. The northern border was placed at 42º21' N, so that the influence on the northern mouth of the presence of the nearby Onza Island is taken into account. The southern border was placed at 42º05' N and the eastern one at the Rande Strait, where the bottom rises sharply from a maximum depth of 20 m up to very shallow waters of about 3 m depth. The model runs with 13 layers, with centres at 2, 5, 8, 12, 17, 25, 35, 45, 55, 65, 75, 85 and 95 meters below the surface. This allows a high degree of vertical resolution at special points like the Rande Strait or the northern mouth. The time step was set to 180 seconds, which is small enough to guarantee stability according to the Courant-Friedrichs-Levy criterion.

Boundary conditions include the aforementioned zero-gradient condition for velocity at the oceanic open border, tidal forcing at that same boundary and velocity conditions at Rande Strait. Tidal forcing is imposed through sea surface elevation at the open boundary, calculated as follows. First, harmonic tidal constants are obtained from tidal registers inside the Ría, providing an initial sea surface level. This is used as a boundary condition (constant all over the open boundary) and corrected down so that bathymetric amplification results in observed values. Finally, amplitude and phase differences between adjacent points of the border are introduced using data from the MARHAM data set (PCM). At Rande Strait velocities are imposed so that San Simón Bay fills and empties correctly with the tide.

The physical forcing processes considered are only tide and wind, and the first one is introduced into the equations via boundary conditions, as explained. Wind forcing is also introduced as a boundary condition of continuity of the stress tensor at the atmospheric interface, so that there the appropriate components match the horizontal wind stress vector.

The horizontal wind stress vector is introduced in the model through the equation:

$$\tau = C_D \rho_a |W| W$$

where $W = (W_x, W_y)$ is the wind velocity near the sea surface, C_D is a dimensionless stress coefficient and ρ_a is the air density. The coefficient C_D is selected according to Smith's criteria (Smith, 1980).

The most representative of the wind data sets available for the model domain is the meteorological station of the INM placed at Cape Finisterre (Figs. 2a and 2b). These data are representative of shelf winds, but not of the winds in the inner part of the Ria. To take into account this difference between external and internal winds, Finisterre winds are imposed uniformly over the shelf and the ría west of Cabo Home and then decreased linearly eastwards from this value down to zero at Rande Strait. This extrapolation of winds was chosen for simplicity,

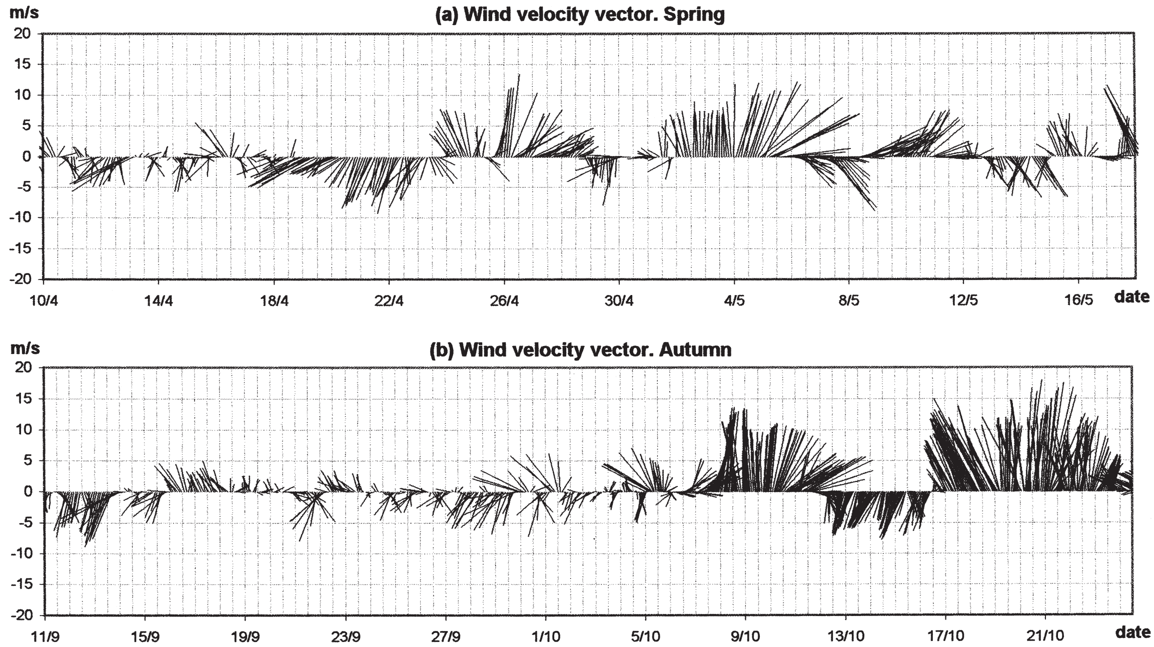

FIG. 2. – Wind from the Finisterre meteorological station for (a) spring and (b) autumn periods.

and is consistent with the observed diminishing of winds, gravity waves and roughness of the sea along the axis of the ría down to Rande Strait.

RESULTS

All results of the model discussed here were obtained with one run of the program over a whole year, covering two periods in which observations are available. An initial warm-up period of two days should be allowed before the simulation data can be compared to real data.

The results presented correspond to the northern mouth of the Ría de Vigo (see Fig. 1), so that $u < 0$ and $v > 0$ (i.e. approximately NW velocity) corresponds to a current which flows out from the Ría, whereas $u > 0$ and $v < 0$ (i.e. approximately SE velocity) corresponds to a current that flows into the Ría.

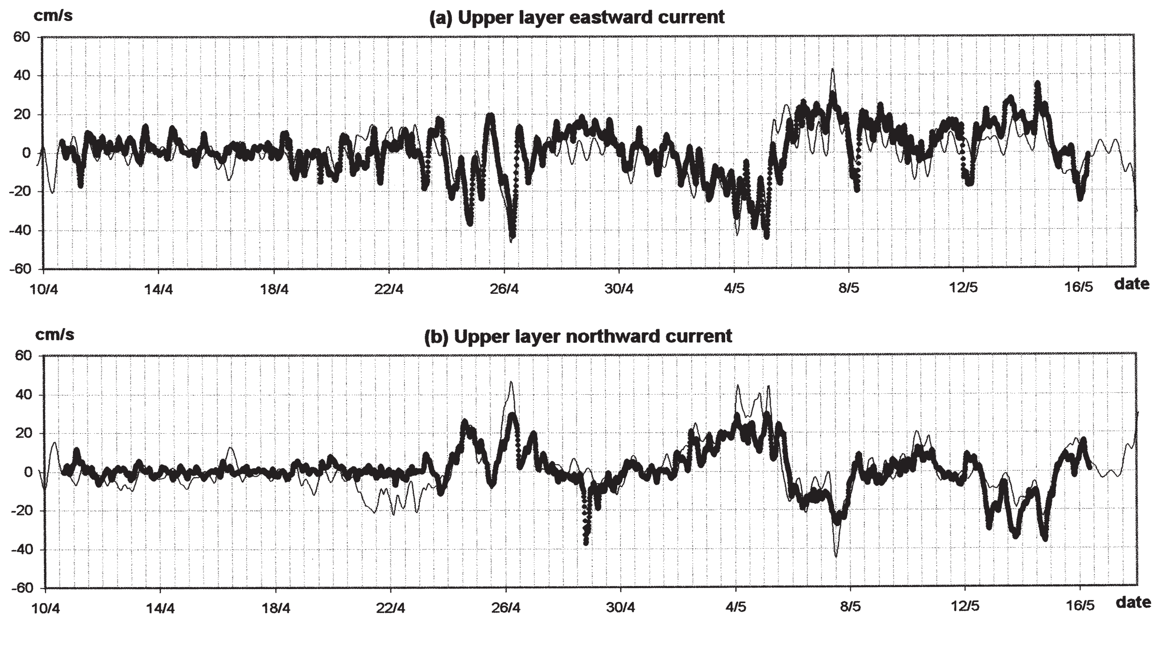

FIG. 3. – (a) Eastward and (b) Northward components of the current at the northern mouth of the Ría de Vigo during the spring period. Solid line depicts model results, dots are measured currents. Values correspond to the upper layer, 0 to 5 m depth.

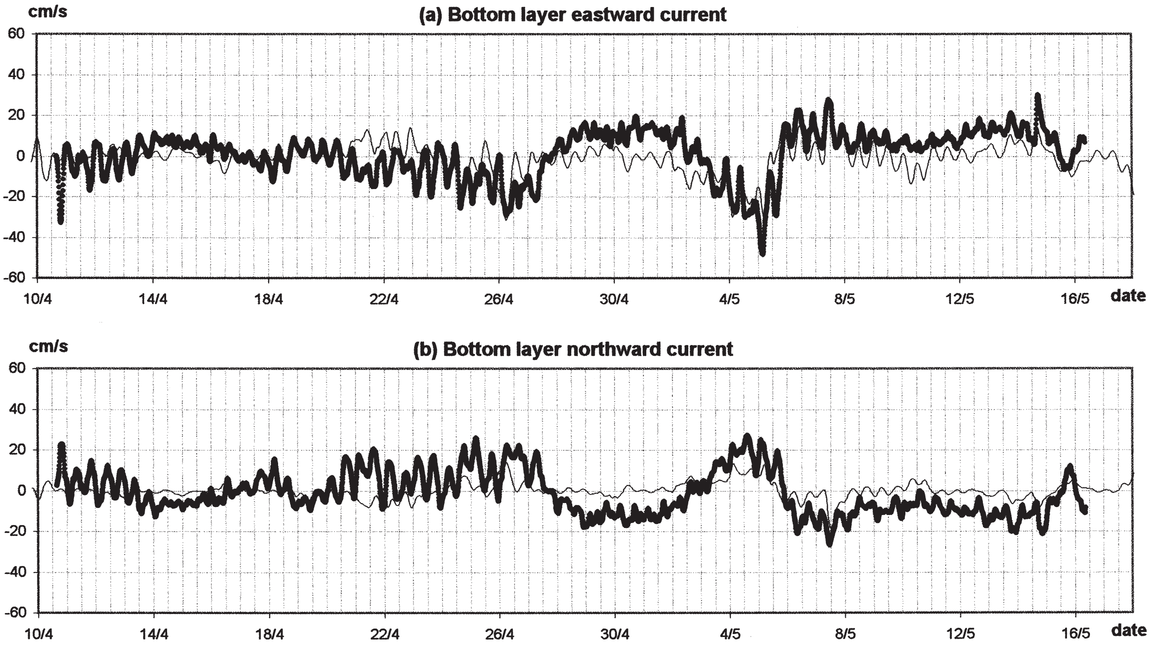

FIG. 4. – (a) Eastward and (b) Northward components of the current at the northern mouth of the Ría de Vigo during the spring period. Solid line depicts model results, dots are measured currents. Values correspond to the bottom layer, roughly 15 to 20 m depth.

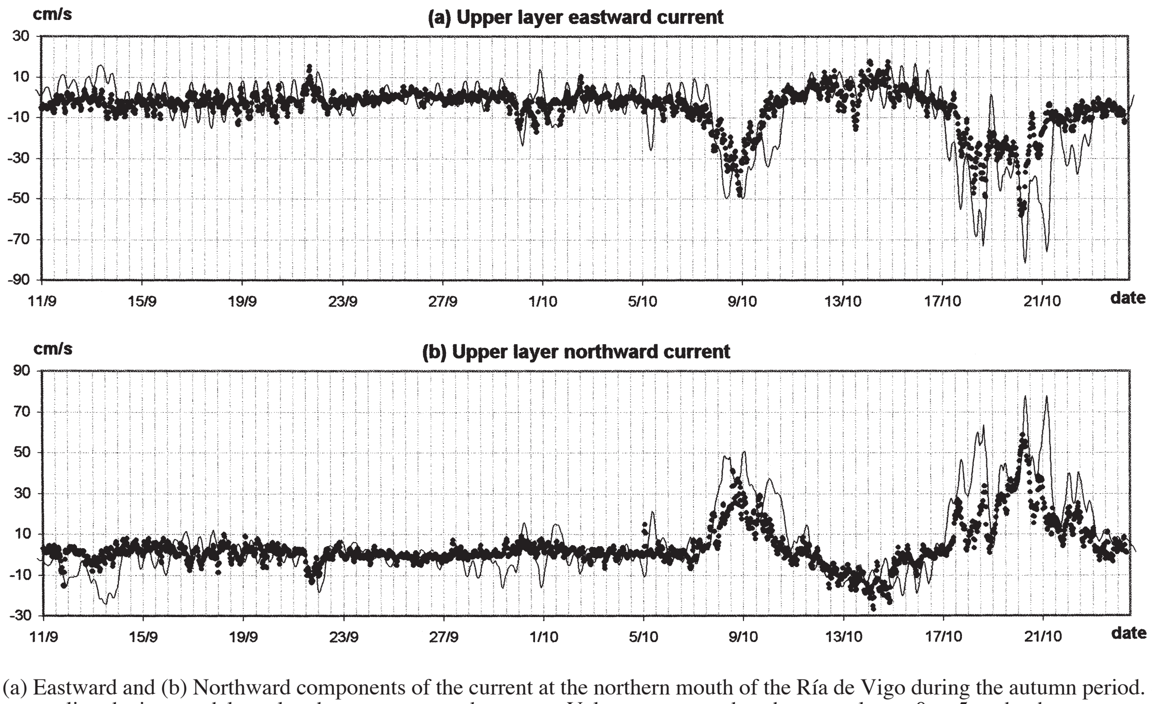

FIG. 5. – (a) Eastward and (b) Northward components of the current at the northern mouth of the Ría de Vigo during the autumn period. Solid line depicts model results, dots are measured currents. Values correspond to the upper layer, 0 to 5 m depth.

The results of the model follow real data both at low (meteorological) frequencies (Figs 3 to 6) and at intermediate (tidal) frequencies (Figs. 7, 8).

The spring period (Figs. 3, 4) has a relatively complex low-frequency structure. After two weeks of little mean movement, various episodes of in- and outflow currents (SE and NW respectively) follow each other, with very different shapes. In some occasions the event is short with energetic diurnal oscillations (e.g. two outflow peaks on 24 and 26 April, diurnal inflows around 14 May), in others it lasts for several days with weak high-frequency oscillations (outflow from April 30 to May 5). The model reproduces this behaviour.

During the autumn period (Figs. 5, 6), in the first four weeks there is no noticeable low-frequency

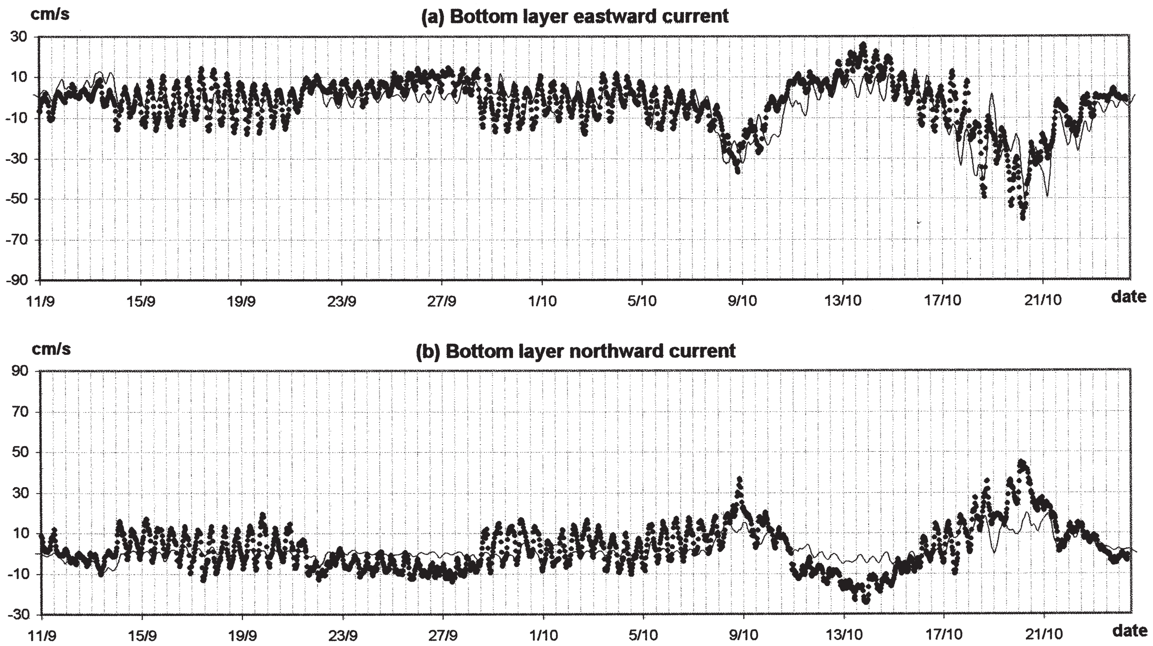

FIG. 6. – (a) Eastward and (b) Northward components of the current at the northern mouth of the Ría de Vigo during the autumn period. Solid line depicts model results, dots are measured currents. Values correspond to the bottom layer, roughly 15 to 20 m depth.

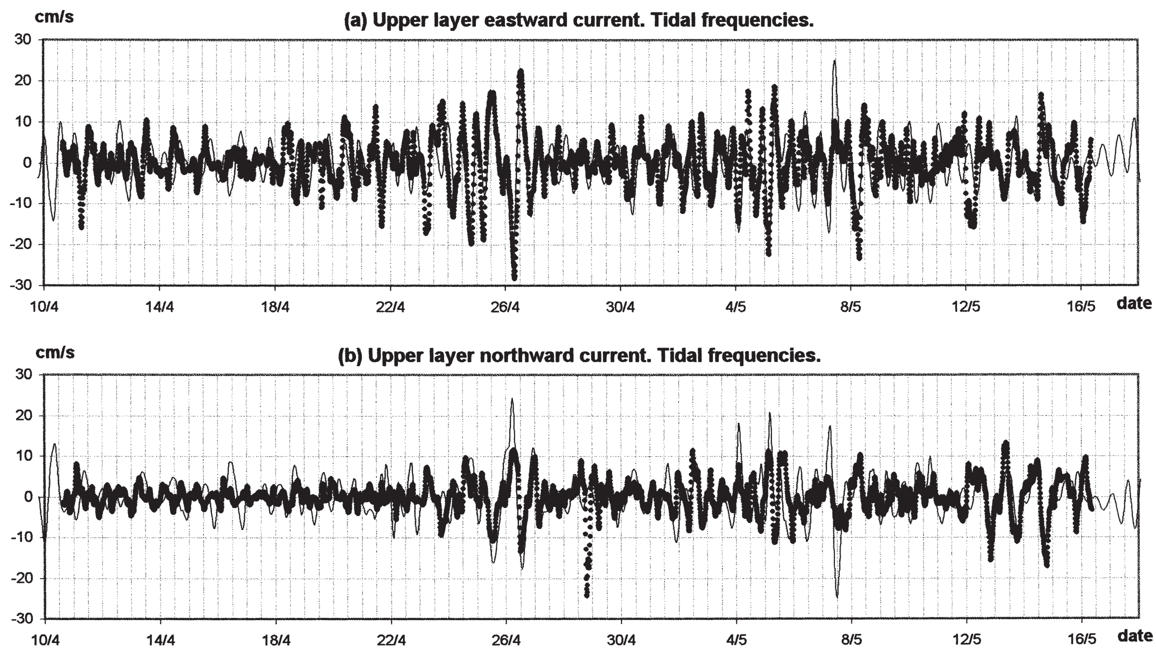

FIG. 7. – (a) Eastward and (b) Northward components of the current at intermediate frequencies at the northern mouth of the Ría de Vigo during the spring period. Solid line depicts model results, dots are measured currents. Values correspond to the upper layer, 0 to 5 m depth.

observed current, and model values are equally close to zero. Then towards the end of the period (9, 18 and 20 October) there appear two pulses of outflow current which the model reproduces well in duration and shape but with higher intensity than that observed.

Model tidal velocities appear to be much more regular than observed ones (Figs. 7, 8). Tidal frequency velocity components have a smooth sinusoidal behaviour in time; observed data are rarely so well-behaved because of the complexity of the real system, including very local winds, small scale turbulence, persistency of inertial movements, etc., which the model at this stage does not attempt to reproduce. However, the correlation

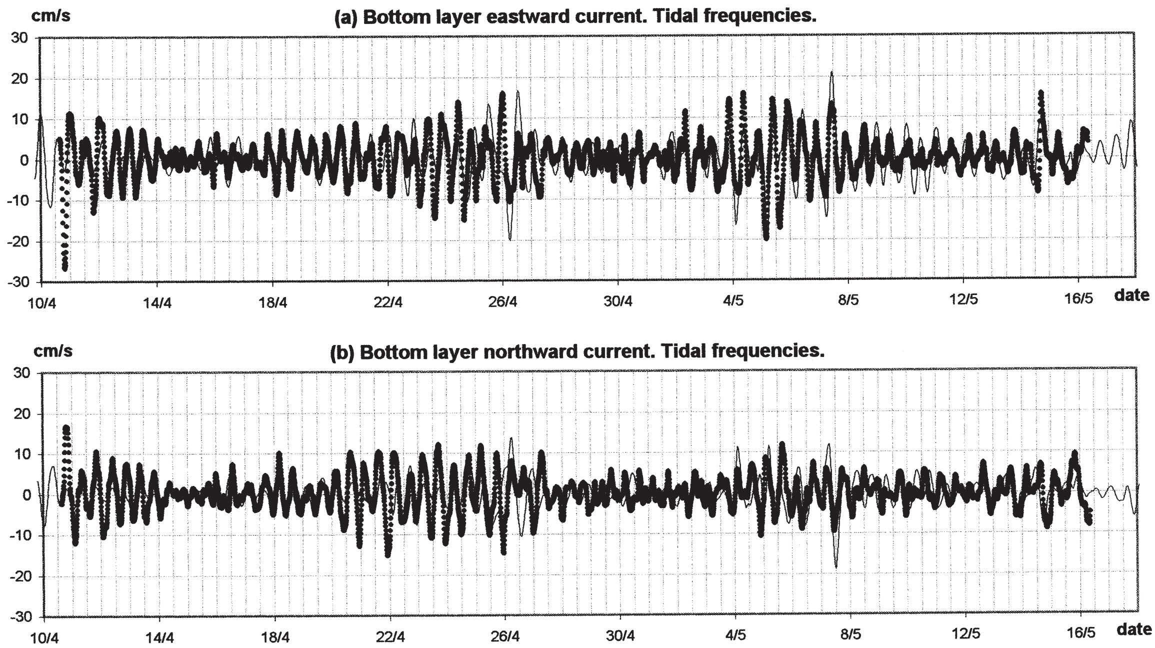

FIG. 8. – (a) Eastward and (b) Northward components of the current at intermediate frequencies at the northern mouth of the Ría de Vigo during the spring period. Solid line depicts model results, dots are measured currents. Values correspond to the bottom layer, roughly 15 to 20 m depth.

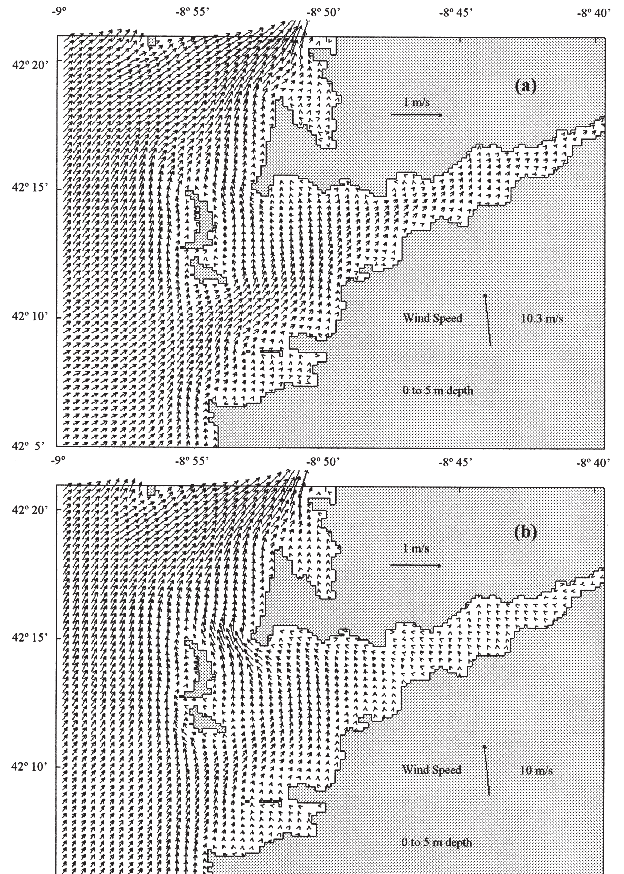

FIG. 9. – Horizontal current velocities at a peak wind speed for the 0 to 5 m layer at (a) 8/10 16:00 (maximum tidal velocities) and (b) 8/10 19:00 (minimum tidal velocities).

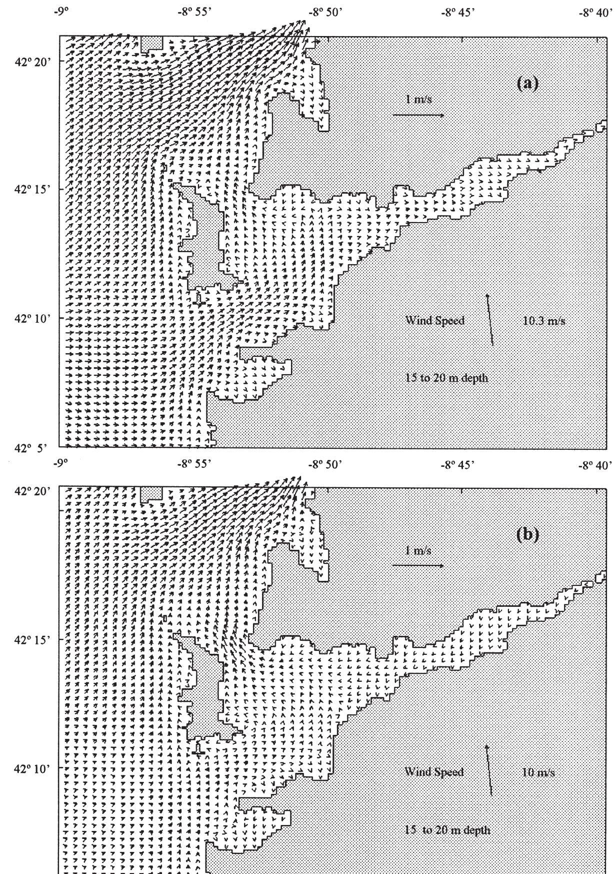

FIG. 10. – Horizontal current velocities at a peak wind speed for the 15 to 20 m layer at (a) 8/10 16:00 (maximum tidal velocities) and (b) 8/10 19:00 (minimum tidal velocities).

between modelled and observed time series is quite noticeable.

Horizontal maps (Figs. 9, 10) show the global circulation pattern during an event of strong southern wind (Oct 8), at two representative depths and at two different tidal phases (4 p.m., mean level at flooding; 7 p.m., high water). The basic circulation consists of an inflow through the southern mouth and an outflow through the northern one. Outflow current at the northern mouth during flooding suggests that wind-generated currents overcome tidal ones, in agreement with experimental data. This wind-driven outflow extends to the whole depth of the northern mouth (see Fig. 10a). The intensity of inflow at the southern mouth diminishes steadily with depth, showing that low frequency currents are in fact outgoing there in the lower part of the section.

This initial application of the model does not account for a complex vertical behaviour of currents: it generally just scales down the surface signal as it propagates it down the water column, whereas the observed behaviour is not always so. In this respect agreement is relatively good in spring and not so good in autumn.

DISCUSSION

The capability of a barotropic version of the HAMSOM three-dimensional finite differences model to predict wind- and tide-driven currents in the Ría de Vigo has been shown.

Generally the model results meander up and down the observed values. The standard deviation of their difference is around 10 cm/s (at low frequencies only 6 cm/s), compared with currents which typically range from minus to plus 30 cm/s. Qualitatively it can be said that the model overestimates low-frequency outflows and underestimates inflows, which is likely to be related to actually how appropriate the wind measured at Cape Finisterre is for calculating currents in the Ría de Vigo. In particular, northerly winds, which are very noticeable at Cape Finisterre, could be screened off by the several peninsulas between it and the Ría de Vigo.

The overall good correlation between the model results and observed currents shows that wind and tide forcing are likely to be the most important factors at time scales of days to weeks, so the appropriate simulation of the currents due to this forcing is the first step before we can reproduce the thermohaline behaviour with a full baroclinic version of the model.

ACKNOWLEDGEMENTS

This work was supported by CICYT Project AMB95-1084-C03, Xunta de Galicia and EU (FEDER Funds).

REFERENCES

Alvarez, E., B. Pérez and I. Rodríguez. – 1997. A description of the tides in the Eastern North Atlantic. *Prog. Oceanogr.*, 40: 217-244.

Backhaus, J.O. – 1983. A semi-implicit scheme for the shallow water equations for application to shelf sea modelling. *Cont. Shelf Res.* 2(4): 243-254.

Backhaus, J.O. – 1985. A three-dimensional model for simulation of shelf sea dynamics. *Deutsche Hydrographische Zeitschrift,* 38(H4): 165-187.

Backhaus, J.O. and D. Hainbucher. – 1987. A finite difference general circulation model for shelf seas and its application to low frequency variability on the North European Shelf. In: J.C.J. Nihoul and B.M. Jamart (eds.), *Three-dimensional models of marine and estuarine dynamics*. Elsevier Oceanography Series, 45: 221-244. Amsterdam.

Rodi, W. – 1980. *Turbulence models and their application in hydraulics*. IAHR state-of-the-art paper. Rotterdam. 104 pp.

Rodríguez, I. and E. Alvarez. – 1991. Modelo Tridimensional de Corrientes. Condiciones de aplicación a las costas españolas y análisis de resultados para el caso de un esquema de mallas anidadas. *Clima Marítimo report*, 42: 65 pp.

Rodríguez I., E. Alvarez, J. Krohn and J.O. Backhaus. – 1991. A mid-scale tidal analysis of waters around the north-western corner of the Iberian Peninsula. *Proc. Computer Modelling in Ocean Eng.* 91, Balkema, 568 pp.

Smith, S.D. – 1980. Wind stress and heat flux over the ocean in gale force winds. *J. Phys. Oceanogr.*, 10: 709-726.

Stronach, J.A., J.O. Backhaus and T.S. Murty. – 1993. An update on the numerical simulation of oceanographic processes in the waters between Vancouver Island and the mainland: the GF8 model. *Oceanogr. Mar. Biol. Ann. Rev.*, 31: 1-86.

Wais, R. – 1985. *On the relation of linear stability and the representation of Coriolis terms in the numerical solution of the shallow water equation*. Ph.D. Thesis, Hamburg University.